IJESKA

contribution to science

International Journal of Earth Sciences Knowledge and Applications

RESEARCH ARTICLE

Characterization of Structural Properties of NiTi Alloys Synthesized by Powder Metallurgy Method

Yunus Tatoğlu[1], Mustafa Engin Kocadağıstan[1*]

[1]Ataturk University, Faculty of Engineering, Department of Metallurgy and Material Engineering, 25400 Erzurum, Turkey

I N F O R M A T I O N

A B S T R A C T

NiTi alloys have shape memory, super elasticity, high impact damping capacity, high corrosion resistance and biocompatibility. Powders with different shapes, sizes and packaging properties can be produced with powder metallurgy methods as high performance, high dimensional sensitivity, chemical composition can be controlled and porous materials. For this purpose, mechanical alloying process was carried out using Ni and Ti powders in equal moles. 58.7g of Ni and 47.9 g of Ti were taken one mole and 0.14 mol of Ni and Ti powders were used in the first three of the experiments. To reduce dust consumption, 0.047 moles of Ni and Ti powders were used in subsequent experiments and it was aimed to obtain a NiTi alloy. The effects of the change of rotational speed and grinding time on alloying were investigated using a planetary grinder. XRD (X-Ray Diffraction) was used for phase analysis. In the planetary grinding device used, the effects of changing the rotation speed and changing the alloying time on alloying were examined. X-ray diffraction graphs and scanning electron microscopy images of NiTi powders synthesized in various parameters were taken and their structural properties were interpreted. In this study, 12 experiments were carried out. The Ti_2Ni phase was not found under 300 rpm and 200 rpm under 40 hours. In 40-hour and 80-hour experiments, peak formation overlapping with Ti_2Ni phase was observed. The Ti_2Ni phase was not found in 10 and 20 hours of experiments at 400 rpm. It was observed that crack formation started in large grains at 400 rpm speed. It was concluded that the experiment period must be at least 40 hours for alloying to take place.

1. Introduction

Powder metallurgy is the process of converting powders with different shapes, sizes and packaging characteristics into high performance and resistant precision parts. Powder metallurgy process steps consist of powder production, mixing of powders, pressing and sintering steps, respectively. If necessary, final surface treatments can be made after sintering. Mixing, alloying and size reduction of powders by mechanical alloying method can be accomplished in a single process. It is possible to produce high purity alloys by preventing contamination with the measures taken. Powder metallurgy (TM) is the most diverse production method among various metal processing techniques. During this process; The mixed or pre-alloyed powders are filled into a mold, pressed as desired, and then the particles are thermally bonded by sintering (Abedini et al., 2010).

The first stage of powder metallurgy is the production of powder. The most important feature of a powder is that its surface area / volume ratio is relatively high. Powders show a behavior between solid and liquid, in this aspect, act like a liquid and can also be compressed. Thus, a metal powder can

be easily delivered to the properties expected from a solid (German, 1984). Knowing how a powder is produced allows the properties of that powder such as shape and size to be predicted at the beginning (Yurtsever, 2014).

In this method, the most preferred method is ball grinders that have high resistance against abrasion and turn with hard balls. In this method, when the ideal speed is achieved, a part of the ball and powder is raised up the upper part of the mill body and the small size powders fall down (Ateş, 2012).

All metals and ceramic parts produced by powder metallurgical method are subjected to sintering at high temperatures in order to provide strength (Kumdali, 2008).

The mechanical alloying method makes it possible to alloy elements that are very difficult or limited to manufacture with traditional production methods. In addition to creating a new composition with this method, it is possible to produce nanoscale particles as a result of long alloying times (Söyler, 2008). Mechanical alloying method is a solid state powder process that involves the welding, breaking and re-welding

processes of particulate powders during high energy grinding (Eskandarany, 2001). With this method, it is possible to produce alloy powders from two or more elemental powders. It also helped to eliminate irregularities that occur during melting and solidification. If the general properties of mechanical alloying are listed (Eskandarany, 2001);

- Fine-dispersed, secondary phase particles can be produced,
- Solid resolution limits can be expanded,
- Reducing grain sizes below nanometer,
- Synthesis of semi-crystalline and new crystalline phases,
- Irregularity of regular intermetallics,
- Development of amorphous phases,
- Elements that are difficult to be alloyed can be alloyed,
- Allows resizing operation.

In mechanical alloying, it is aimed to form a homogeneously dispersed structure by mixing two or more elemental powders. It is a solid phase technique that involves cold welding, breaking and subsequent re-welding of dust particles thanks to high energy grinding. Dust particles between the two balls colliding in this grinding undergo plastic deformation. As this process continues, the particles become flat, cold welded, broken and re-welded (Eskandarany, 2001).

The most popular grinders used in mechanical alloying are "planet type" grinders. The supporting discs keep the chambers in the opposite direction of movement, while the chambers rotate about their axis. In this way, the centrifugal force inside the sleeve changes direction every half turn. The grinding balls roam very quickly and hit the opposite wall. The dust remaining between the balls or between the ball and the wall is ground by impact (Efendi, 2017).

NiTi alloys have wide usage areas thanks to their shape memory feature, superelasticity, high corrosion resistance, lightness, high impact damping capacities and can be produced in porous structure (Akhlaghi et al., 2011).

The approximately equimolar Ni-Ti alloy, called nitinol, is the most widely used shape-memory alloy (Novák, et al., 2017) Shape memory alloy systems with the most commercial value in the industry are NiTi alloys and copper based alloys (Dikici, 2010). NiTi alloys are binary and coatomic intermetallic alloy systems. In pure metals, atoms are bonded together by a metallic bond. In intermetallic components, binding occurs in a covalent nature. The crystal structures of intermetallics differ from the crystal structure of the elements that make up itself (McNeese et al., 2000).

The most reliable phase diagram of NiTi alloys is given by Otsuka and Ren (2005). In this diagram, eutectoid transformation is observed at 630 °C. Although pure titanium melting temperature is 1670 °C and pure nickel melting temperature is 1455 °C, the melting temperature of NiTi alloy is 1310 °C. When the intermetallic NiTi structure reaches 630 °C, the NiTi intermediate phase is formed. The resolution of the Ni element in this phase increases from 700 °C to 1183 °C and reaches a maximum value of 55% (Eroğlu, 2010).

Ti_3Ni_4 precipitates are observed in the form of thinly dispersed fine spots in the matrix formed after the aging process applied below 550 °C to the alloy taken into solution at 800 °C -900 °C. These deposits are of great importance in the alloy's bidirectional shape memory feature (Otsuka and Wayman, 1998; Yurtsever, 2014; Tatoğlu, 2019).

In this study, it is aimed to obtain NiTi alloy by mechanical alloying from TM methods. In the planetary grinding device used, the effects of changing the rotation speed and changing the alloying time on alloying were examined. The X-ray diffraction graphs and scanning electron microscopy images of NiTi powders synthesized in various parameters were taken and their structural properties were interpreted.

2. Materials and Methods
2.1. The NiTi powder
The powders used are alloyed in equal mole ratio and their weight values are calculated below;

$$n = m/Ma \qquad (1)$$

In the formula; n is the number of moles, m is mass and Ma: refers to the atomic weight.

1 mole of Ni is 58.7 g and 1 mole of Ti is 47.9g. So, 47,9 g Ti powder should be added to 58,7 g Ni powder. When proportioned from here;

- 6.73 g Ti powder to 8.25 g Ni powder,
- 2.23 g Ti powder should be used for 2.75 g Ni powder.

In the first three of the experiments, 0.14 mol Ni and Ti powders were used. 0.047 moles of Ni and Ti powders were used in subsequent experiments to reduce dust consumption.

2.2. Atmosphere Controlled Powder Mix
In order to protect the elements from the oxygen atmosphere due to the oxidation sensitivity of the elements, the process of taking the powders into the chamber was made in the glove box (Atmosphere Controlled Powder Mix). Oxidation or contamination in the elements is prevented thanks to the glove box, which contains an argon environment. Argon gas was used as a working environment.

2.3. Mechanical alloying
As an alternative to conventional production methods for the NiTi alloy, powder-metallurgy processes starting from pre-alloyed NiTi powder have been developed. Mechanical alloying is one of the techniques used for the production of nano-structured powders (Novák, et al., 2017).

In this study, Retsch Planetary Ball Mill PM100 was used to make mechanical alloying. The PM 100 is a convenient benchtop model with 1 grinding station. Material feed size; < 10 mm and final fineness; < 1 µm, for colloidal grinding < 0.1 µm. W x H x D closed; 640 x 480 (780) x 420 mm. Using the Ti and Ni elements in equal molar ratios, Retsch PM100 brand planetary ball mill and tungsten carbide chamber and balls were mechanically alloyed with the parameters in Table 1. These experiments were carried out by changing the speed

and time by keeping the other parameters constant. In all experiments, the ball: sample ratio was set to 10:1. In the completed experiments, the removal of the dust from the chamber was done in an argon environment glove box. In addition, 0.5% stearic acid (SA) was used in all experiments to prevent chamber and ball plastering. In experiment 1, 8.25g Ni and 6.73g Ti powders were put into the chamber and operated for a total of 1 hour with 15 minutes of operation at 300 rpm and 1 minute of pause. All experiments in the table has been studied with this system.

Table 1. The experiment parameters

| No	Sample (g)	Time (h)	Working Range (min)	Halt (min)	Speed (rpm)	Ball/Sample	Reservoir/Ball
1	Ni (8,25)Ti (6,73)SA (0,07)	1	15	1	300	10:1 (150g:15g)	Tungsten Carbide (19 pieces-150g)
2	Ni (8,25)Ti (6,73)SA (0,07)	2	15	1	300	10:1 (150g:15g)	Tungsten Carbide (19 pieces-150g)
3	Ni (8,25)Ti (6,73)SA (0,07)	3	15	1	300	10:1 (150g:15g)	Tungsten Carbide (19 pieces-150g)
4	Ni (2,75)Ti (2,23)SA (0,05)	1	15	5	200	10:1 (50g:5g)	Tungsten Carbide (6 pieces-50 g)
5	Ni (2,75)Ti (2,23) SA(0,05)	2	15	5	200	10:1 (50g:5g)	Tungsten Carbide (6 pieces-50 g)
6	Ni (2,75)Ti (2,23)SA (0,05)	3	15	5	200	10:1 (50g:5g)	Tungsten Carbide (6 pieces-50 g)
7	Ni (2,75)Ti (2,23)SA (0,05)	10	15k	5	200	10:1 (50g:5g)	Tungsten Carbide (6 pieces-50 g)
8	Ni (2,75)Ti (2,23)SA (0,05)	20	15	5	200	10:1 (50g:5g)	Tungsten Carbide (6 pieces-50 g)
9	Ni (2,75)Ti (2,23)SA (0,05)	40	15	5	200	10:1 (50g:5g)	Tungsten Carbide (6 pieces-50 g)
10	Ni (2,75)Ti (2,23)SA(0,05)	80	15	5	200	10:1 (50g:5g)	Tungsten Carbide(6 pieces -50 g)
11	Ni (2,75)Ti (2,23)SA(0,05)	10	15	5	400	10:1 (50g:5g)	Tungsten Carbide(6 pieces -50 g)
12	Ni (2,75)Ti (2,23)SA (0,05)	20	15	5	400	10:1 (50g:5g)	Tungsten Carbide(6 pieces -50 g)
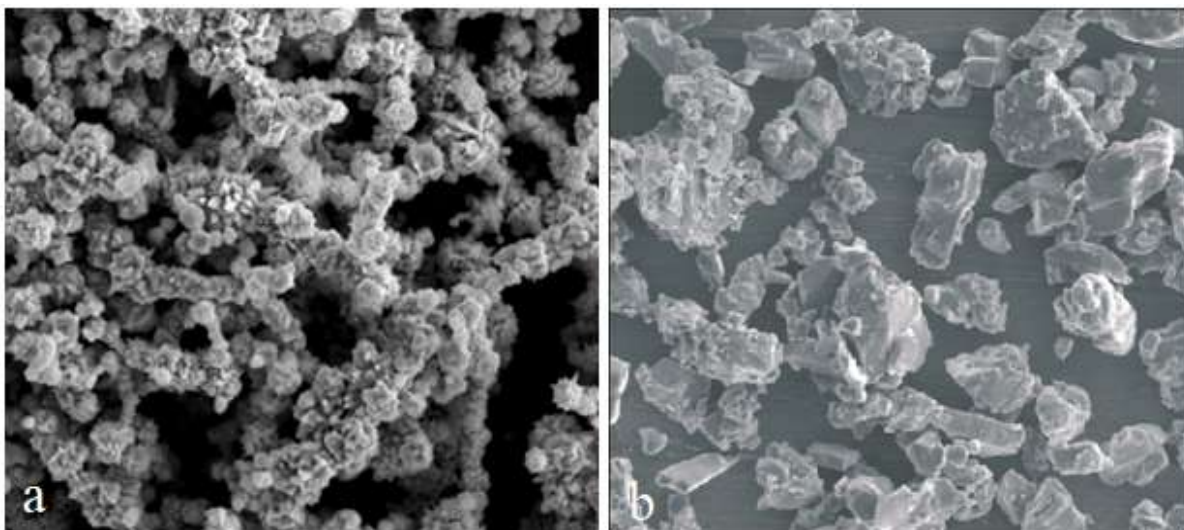
Fig. 3. SEM images of Ni (a) and Ti (b) powders

2.4. Vibrating sieve machine
In order to classify the dusts to the desired size, the sieve was used in the Retsch brand Horizontal Sieve Shaker AS 400 control model. To make the dimensions homogeneous for the samples with mechanical alloy treatment, a 15-minute sieving process was performed on the vibrating screen using 45-micron size sieves.

2.5. X-Ray Diffraction (XRD) analysis
With X-ray measurements, information about the phases, amount of phases, crystal size, mesh parameters, changes in structure, crystal orientation and atom positions can be obtained without damaging the crystal structure in the material. The structural analysis of samples was performed with Bruker D2 Phaser X-Ray Diffractometer.

The XRD measurements were performed from the Cu-Kα source at a wavelength of $\lambda = 1.54184$ A°, 20-100 ° scanning range, 2 degree / min scanning speed and 0.026 degree scanning step. The reflection peaks obtained were compared with the existing the Joint Committee on Powder Diffraction Standards (JCPDS) file.

2.6. SEM and EDS analysis

The surface characterization and elemental analysis of the samples were done with the FEI brand QUANTA FEG 450 model SEM device. SEM images were taken at 1000, 3000, 5000, 10000 and 25000 magnifications separately and their grain structures were examined. Then, whether homogeneity was achieved in the structure was checked by the EDS analysis.
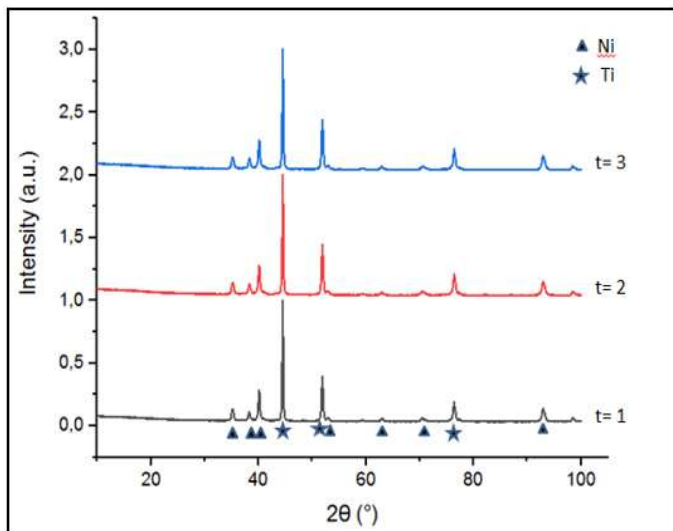

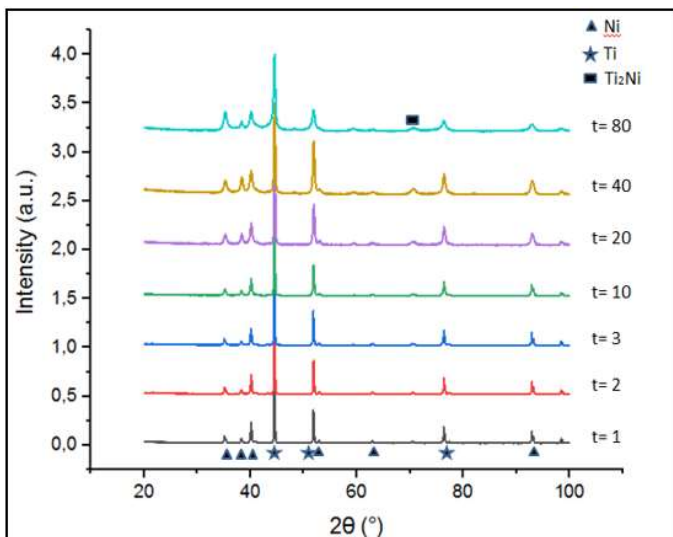Fig. 2. The X-ray diffraction graph of mechanically alloyed powders for 1, 2 and 3 hours

Fig. 3. The X-ray diffraction graph of mechanically alloyed powders for 1, 2, 3, 10, 20, 40 and 80 hours

3. Results and Discussion
3.1. Pure Ni-Ti powders and X-Ray Diffraction analysis

During spark-plasma sintering of the mechanically alloyed powder, the Ni_4Ti_3, Ni_3Ti and monoclinic NiTi develop. Due to this fact, the formation of the undesirable Ti_2Ni phase cannot be avoided (Novák, et al., 2017). SEM images of Ni and Ti elemental powders are given in Fig. 1. As can be seen from the images, Ti particles are 45-50 μm in size and have

no specific form. Ni particles have a global morphology and uniform structure.
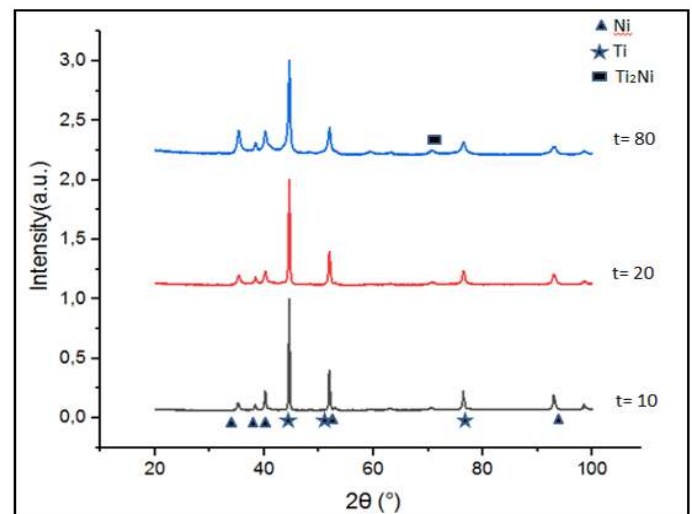

Fig. 4. The X-ray diffraction graph of mechanically alloyed powders for 10 and 20 hours at 400 rpm and 80 hours at 200 rpm.

XRD patterns of Ni-Ti dusts are shown in Figs. 2 and 3. In Fig. 2, phase analysis of the dust collected per hour without stopping the device for 1, 2 and 3 hours at 300 rpm is given. According to this analysis, similar conditions were obtained in peak intensities in the first 1, 2 and 3 hours of mechanical alloying process.
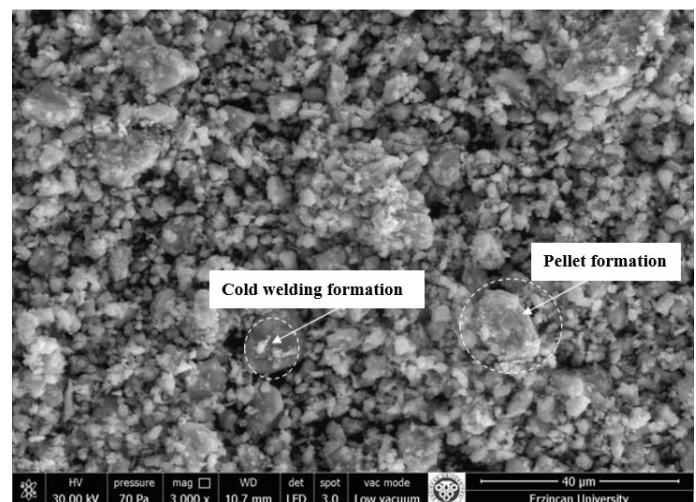

Fig. 5. Cold welding formation and pellet formation

Taking a certain amount of sample from the hopper per hour without stopping the process was not considered effective due to the oxidation sensitivity of the elements. In other studies, the device was operated for the amount of hours to be applied and samples were taken from the chamber. In the Fig. 3, phase analyzes of mechanically alloyed powders are given at 1, 2, 3, 10, 20, 40 and 80 hours at 200 rpm. According to this analysis, similar intensities in peak intensities were obtained in the first 1, 2 and 3 hours of mechanical alloying process.
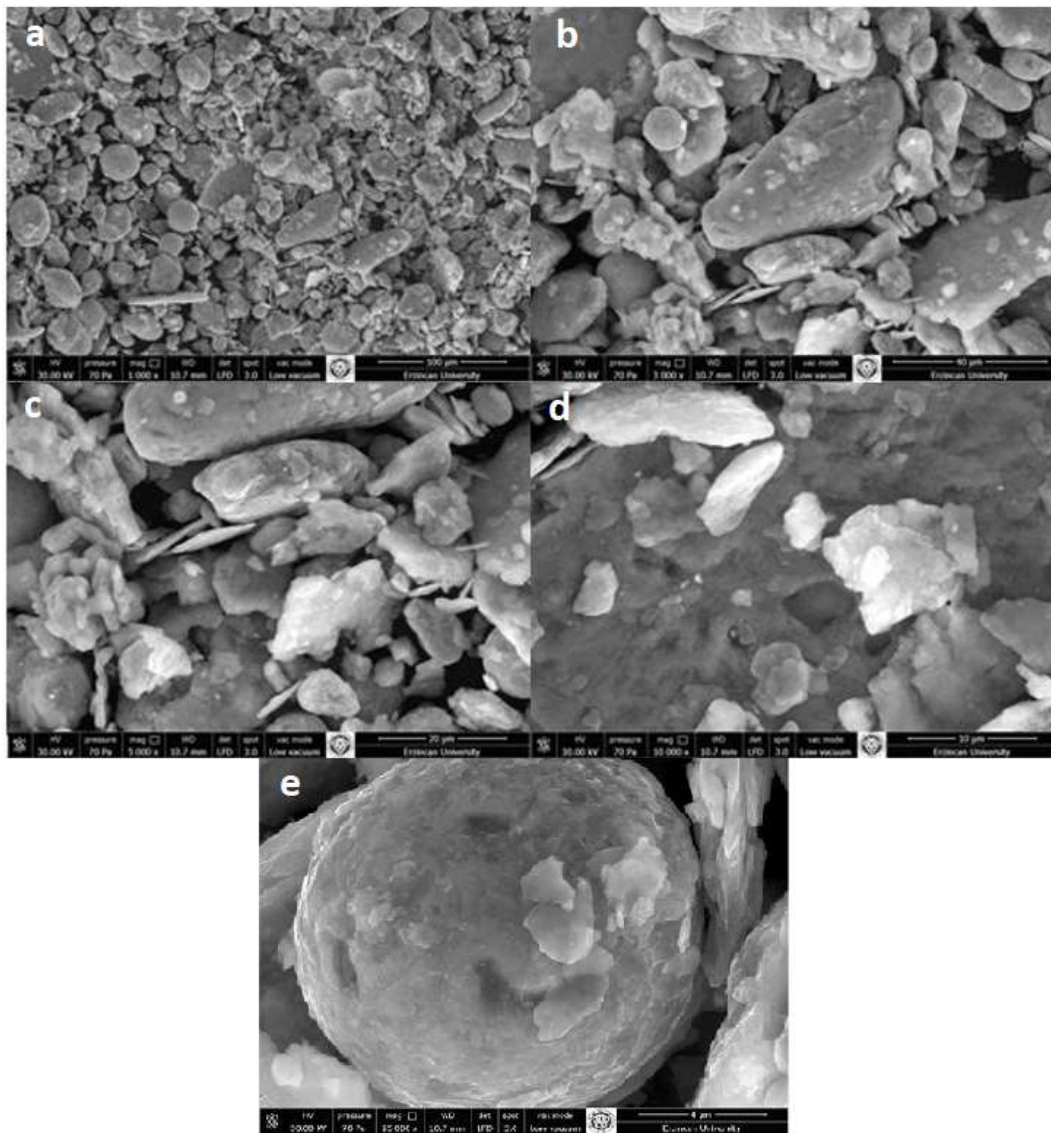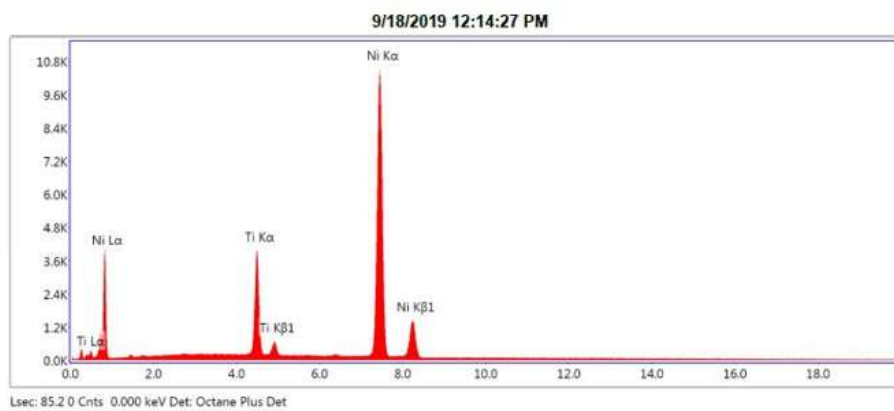
Fig. 6. 10 hours 400 rpm ((a): x1000, (b): x3000, (c): x5000, (d): x10000 and (e): x25000)) SEM images

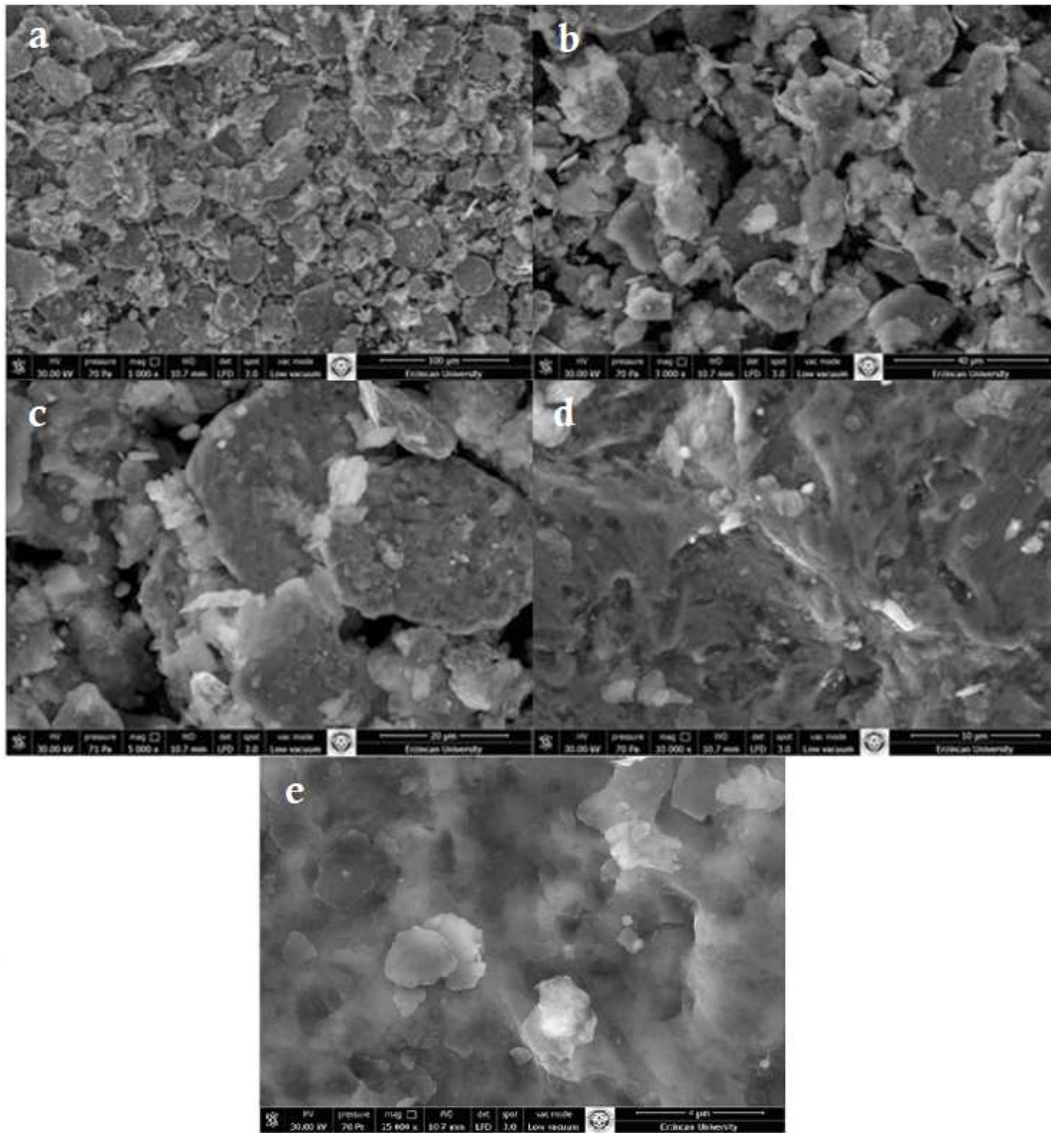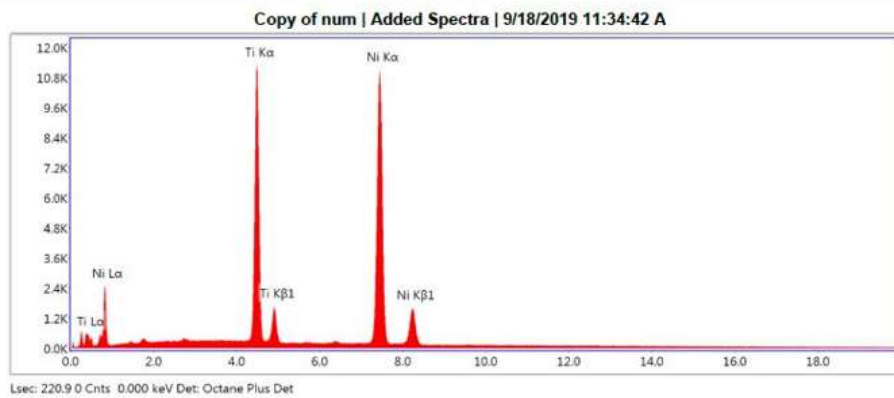| Element	Weight %	Atomic %	Net Int.	Error %
TiK	13.46	16.01	529.25	2.95
NiK	86.54	83.99	1844.15	1.48

Fig. 7. 10 hours 400 rpm EDS analysis

Fig. 8. 20 hours 200 rpm ((a):x1000, (b):x3000, (c):x5000, (d):x10000, (e):x25000)) SEM images

Element	Weight %	Atomic %	Net Int.	Error %
TiK	30.32	34.79	600.5	2.2
NiK	69.68	65.21	748.97	1.76

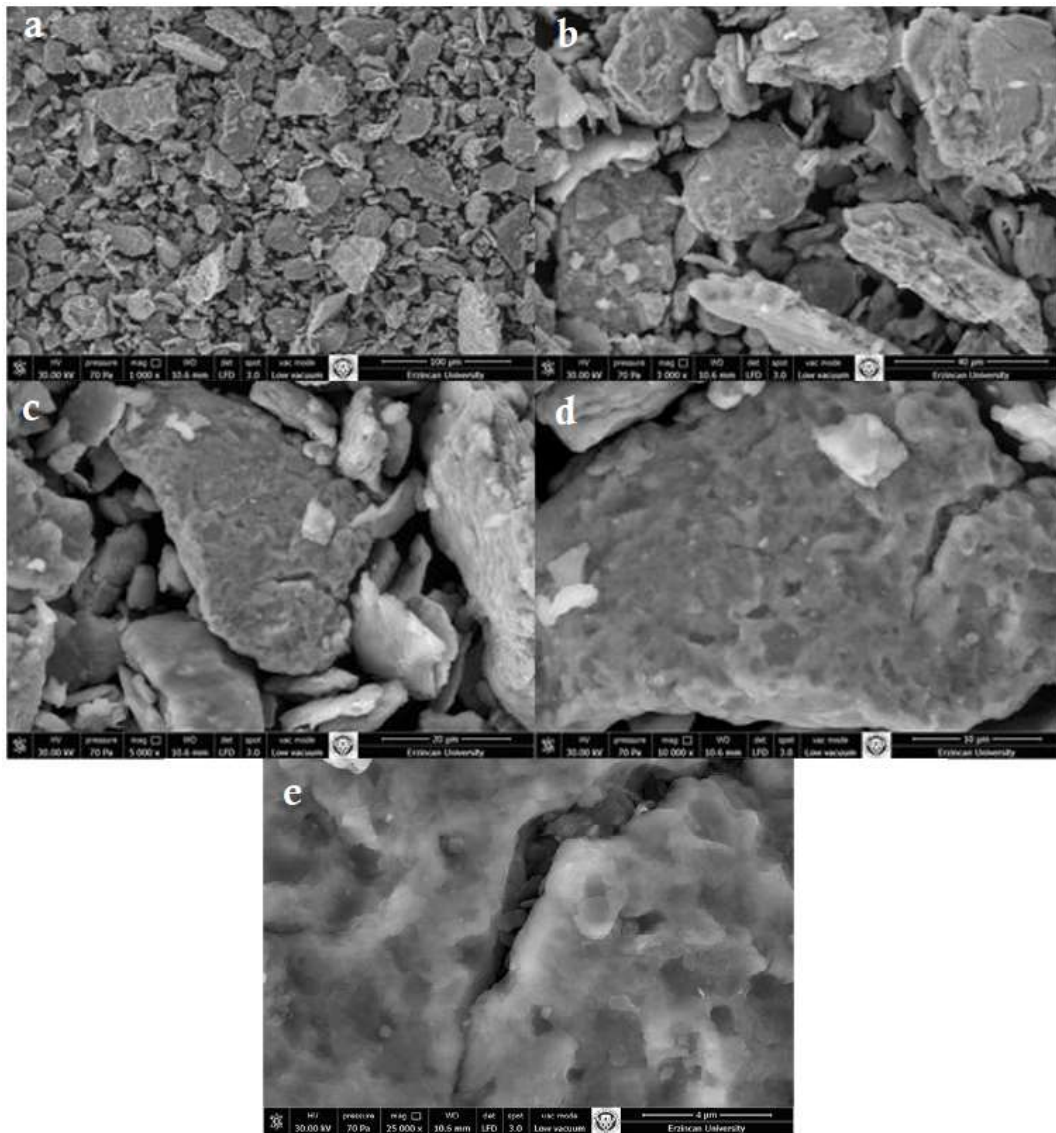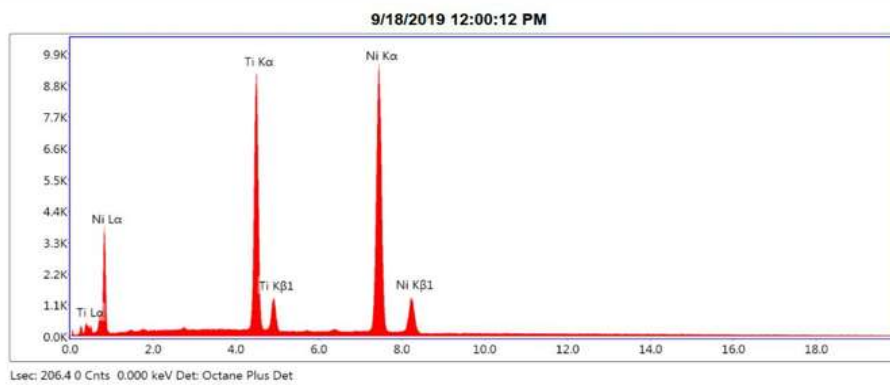Fig. 9. 20 hours 200 rpm EDS analysis

Fig. 10. 20 hours 400 rpm ((a): x1000, (b): x3000, (c): x5000, (d): x10000 and (e): x25000)) SEM images

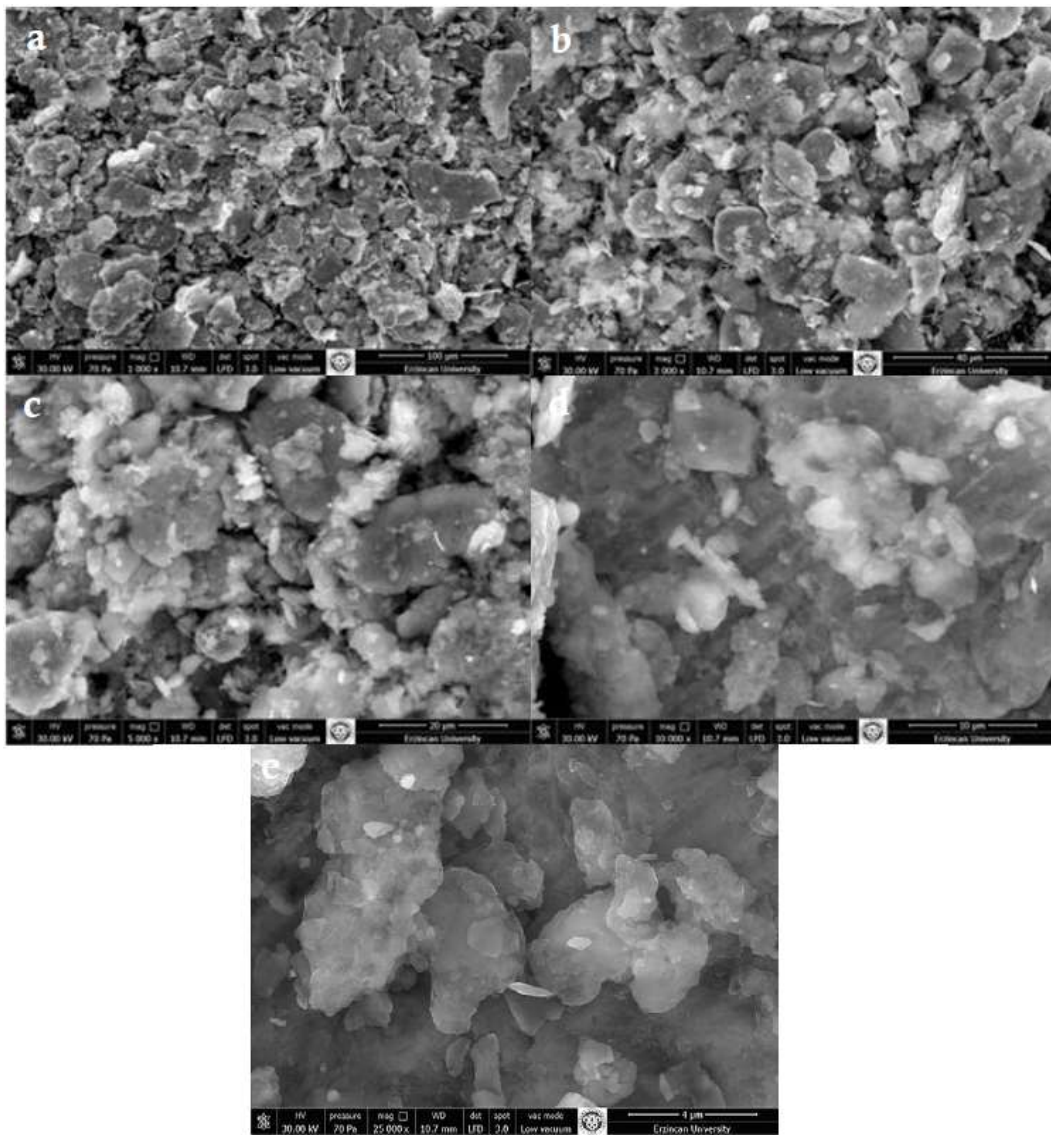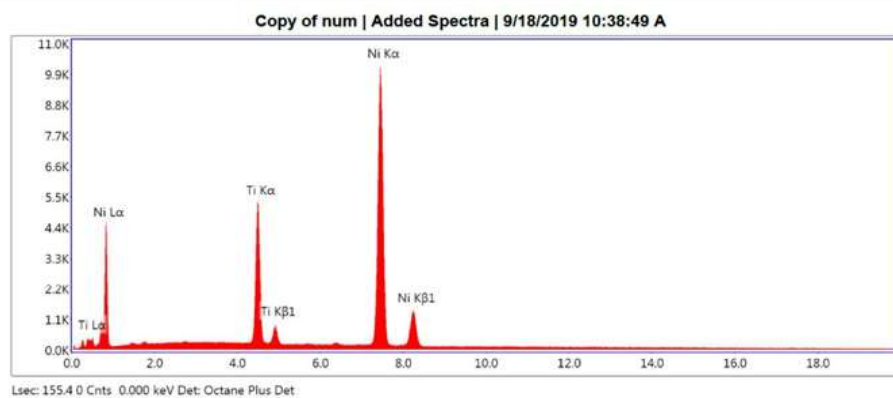| Element	Weight %	Atomic %	Net Int.	Error %
TiK	29.52	33.92	527.32	2.26
NiK	70.48	66.08	683.63	1.77

Fig. 11. 20 hours 400 rpm EDS analysis

Fig. 12. 40 hours 200 rpm ((a): x1000, (b): x3000, (c): x5000, (d): x10000 and (e): x25000)) SEM images

Fig. 13. 40 hours 200 rpm EDS analysis
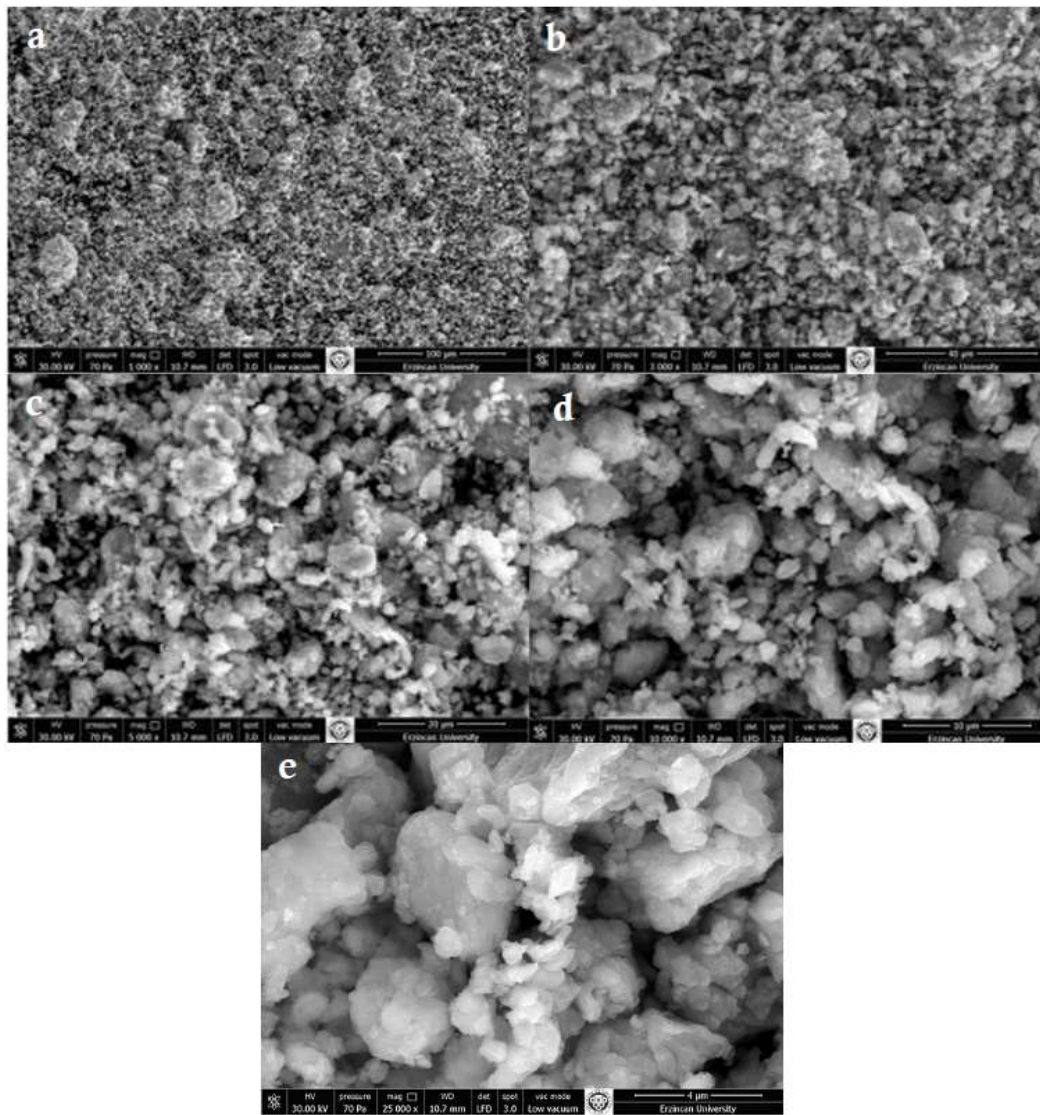
Fig. 14. 80 hours 200 rpm ((a): x1000, (b): x3000, (c): x5000, (d): x10000 and (e): x25000)) SEM images
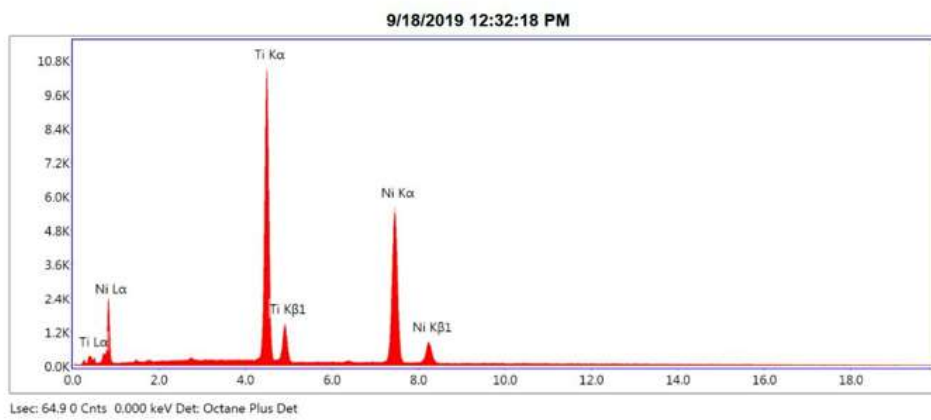
Element	Weight %	Atomic %	Net Int.	Error %
TiK	44.53	49.59	1922.91	1.95
NiK	55.47	50.41	1283.33	2.13

Fig. 15. 80 hours 200 rpm EDS analysis

It was observed that peak intensities decreased and an amorphous structure was observed as the processing time increased. The peaks obtained in the first forty hours of mechanical alloying are compatible with nickel and titanium peaks and no peaks to form a phase have yet been observed. After the 40th hour of mechanical alloying, an additional XRD peak overlapping the Ti_2Ni phase was obtained. Ni peaks have been completely clarified and cubic structure can be defined.

After one-hour grinding process, the peaks characterizing Nickel and Titanium were clearly observed, but when this period was compared with the literature, it was understood that there was not enough time for Ni-Ti alloy formation. Similarly, there was no significant change in XRD peaks in 2 and 3 hour processes. However, due to the increased grinding times, decreases in Ni and Ti phase densities and increases in peak widths were also observed. This has become more evident especially in the 80-hour grinding period. The weakening of the Ti peak and the shifting of Ni to low angles indicate that the Ti atoms diffuse into the Ni lattice system.

In another study, changes were made to the speed values. The graph in Fig. 4 shows the X-ray diffraction graph of mechanically alloyed powders for 10 and 20 hours at 400 rpm and 80 hours at 200 rpm.

The similar peaks were obtained for 10 and 20 hours of experiments at 400 rpm and 10 and 20 hours of experiments at 200 rpm. The XRD peak, seen at 80 rpm at 200 rpm and overlapping the Ti_2Ni phase, was not found in experiments at 10 and 20 hours at 400 rpm. In other experiments, it is envisaged to increase the experiment time at 400 rpm and obtain different phases.

3.2. SEM and EDS analysis of NiTi powders

The SEM and EDS images of ground NiTi powder particles after a series of grinding processes are given below (Figs. 5, 6 and 7). As can be seen from the figures, a lamellar structure is observed at the beginning of mechanical alloying. During grinding, cold welding is observed between the laminates of the soft parts. This lamellar structure is thought to be formed due to the continuous cold welding between laminates during the grinding process of ductile parts. The particle size decreases with longer mechanical alloying time. Because the increase in brittleness causes the formation of smaller particles in granular forms. In other words, continuous cold welding and breaking processes have resulted in a pellet formation formed by nanoscale Ni and Ti particles.

Looking at the SEM images of the alloying made at a speed of 400 rpm for 10 hours, it is seen that the breaking events have not started yet. It is understood from the EDS analysis that homogeneity has not been provided yet. Time should be increased in order to ensure the alloying process and to obtain a homogeneous structure.

According to EDS analysis, it is seen that alloying does not occur in mechanical alloying performed at 200 rpm for 20 hours (Figs. 8 and 9). It is understood that cold welding and breaking events have not yet created a balance. However, when the SEM images are compared with the alloying lasting

for 10 hours, there is a reduction in the dust necks. From this, it is concluded that refraction events begin in fine powders. Longer times are required to achieve alloying and obtain a homogeneous structure.

It has been understood that a homogeneous structure has not yet been formed in the SEM images of the mechanical alloying made at a speed of 400 rpm for 20 hours (Figs. 10 and 11). Time was not enough for the balance of cold welding and breakage. Smaller grains are seen compared to alloying lasting 10 hours. It is understood that the breakage started in fine grains from here. It is seen that cracks start in large grain powders in the microstructure.

The grinding time over 40 hours caused the purification of layered microstructures (Figs. 12 and 13). Therefore, the particles break and continuous cold welding occurred. Very fine microstructural formations were observed in the Ni and Ti layers. The formation of these microstructures with multi-faceted interfaces between layers and increasing grinding time and decreasing the thickness of the layers increase the interaction between the layers. As a result, it leads to homogeneous microstructure formation at longer grinding times.

According to EDS analysis, the sample had a homogeneous structure, especially after 80 hours of grinding (Figs. 14 and 15). It is in good agreement with the nominal compound composition. In other words, the elemental distribution of Ni and Titanium was found satisfactory. Ti is also scattered throughout the Ni matrix, which confirms the homogeneous structure formation.

4. Conclusions

In this study, a total of 12 experiments were completed. The following results were obtained in repeated experiments by changing the rotation speed and alloying times;

- Sampling per hour in experiments repeated at 300 rpm did not yield positive results and caused oxidation. In addition, Ti_2Ni phase did not occur in experiments lasting up to 3 hours at 300 rpm. In the ongoing experiments, it was deemed appropriate not to take samples until the duration of the experiment was completed.
- In experiments repeated at a speed of 200 rpm, Ti_2Ni phase was not found under 40 hours of experiment time. In experiments lasting 40 hours and 80 hours, peak formation overlapping with Ti_2Ni phase was observed.
- In experiments repeated at 400 rpm, test times were set as 10 and 20 hours, but Ti_2Ni phase was not found.
- Comparing SEM images that occurred at 200 rpm and 400 rpm in 20-hour experiments, it was observed that crack formation began in large grains at 400 rpm speed. It was concluded that increasing the rotational speed from here increases the breaking events.
- Since the Ti_2Ni phase is only obtained at 200 rpm, the effect of the rotation speed on the alloy has not been determined. However, it was concluded that the experiment period should be at least 40 hours for alloying to take place.

- The samples achieve much higher mechanical properties than a NiTi alloy produced by the conventional route, but they exhibit almost brittle behavior. This can be caused by the change of deformation mechanism when going to the nanoscale, or by trace contamination of the grain boundaries during the mechanical alloying process, lowering the cohesion of the grains (Novák, et al., 2017).
- In addition, studies can be conducted to investigate the usability of powders in this study in medicine (orthopedics) and dentistry (orthodontics) after pressing and sintering the powders using the cold isostatic press.

References

Abedini, M., Ghasemi, H.M, Nili-Ahmadabadi, M., 2010. Tribological behavior of NiTi alloy against 52100 steel and WC at elevated temperatures. Materials Characterization 61, 689-695.

Akhlaghi, M., Mahmudi, R., Nili-Ahmadabadi, M., 2011. Deformation energy of NiTi shape memory wires. Materials and Design 32, 1923-1930.

Ateş E.A., 2012. Application of aging heat treatment to AA2014-Al4C3 systems produced by powder metallurgy and investigation of their microstructural properties. Master's Thesis (in Turkish) Gazi University, Graduate School of Natural and Applied Science, Ankara, Turkey.

Dikici, B., 2010. Manufacturing of nickel titanium alloys by the powder metallurgy method. Master's Thesis (in Turkish) Istanbul Technical University, Graduate School of Natural and Applied Science, Istanbul, Turkey.

Dilibal, S., 2005. Manufacturing of nickel-titanium shape memory alloy and shape memory training. PhD Thesis (in Turkish) Yildiz Technical University, Graduate School of Natural and Applied Science, Istanbul, Turkey.

Efendi, E., 2017. Sintering and characterization of Ti-5Al-2,5Fe-xCu-yAg alloys produced by mechanical alloying. Master's Thesis (in Turkish) Kocaeli University, Graduate School of Natural and Applied Science, Kocaeli, Turkey.

Eroğlu, E.Z., 2010. Production of shape memory alloys (nickel base and other base) by ark melting, investigation of their metallurgical. Master's Thesis (in Turkish) Dokuz Eylul University, Graduate School of Natural and Applied Science, Izmir, Turkey.

Eskandarany, M. S., 2001. Mechanical Alloying for Fabrication of Advanced Engineering Materials, Mississippi University Press, 257p, New York, USA.

German, R.M., 1984. Powder Metallurgy Science, Metal Powder Industries Federation, 105p, New Jersey, Princeton.

Kumdalı, F., 2008. The production of aluminum based composites with B4C by powder metallurgy. Master's Thesis (in Turkish) Yildiz Technical University, Graduate School of Natural and Applied Science, Istanbul, Turkey.

McNeese, M.D., Lagoudas, D.C., Pollock, T.C., 2000. Processing of TiNi from elemental powders by hot isostatic Pressing. Materials Science and Engineering A 280,334-348.

Novák, P., Moravec, H., Vojtìch, V., Knaislová, A., Skoláková, A., Kubatík, T. F., Kopecek J., 2017. Powder-Metallurgy Preparation of NiTi Shape-Memory Alloy Using Mechanical Alloying and Spark-Plasma Sintering. Materiali in Tehnologije / Materials and Technology 51 (1), 141-144.

Otsuka, K. Wayman, C.M., 1998. Shape Memory Materials, Cambridge University Press.

Otsuka, K., Ren, X., 2005. Physical metallurgy of Ni-Ti-based shape memory alloys. Progress in Materials Science 24, 511-678.

Söyler, A. U., 2008. Development and characterization of Al-Fe based SiC and Y2O3 reinforced composites developed via mechanical alloy. Master's Thesis (in Turkish) Istanbul Technical University, Graduate School of Natural and Applied Science, Istanbul, Turkey.

Tatoğlu, Y., 2019. The characterization of structural properties of NiTi alloys synthesized by powder metallurgy method. Master's Thesis (in Turkish) Ataturk University, Graduate School of Natural and Applied Science, Erzurum, Turkey.

Yurtsever, Ö., 2014. Powder state synthesis of different compositions in Ni-Ti system via mechanical alloying and their characterization after sintering. Master's Thesis (in Turkish) Istanbul Technical University, Graduate School of Natural and Applied Science, Istanbul, Turkey.